SEISMIC RESIDUAL CAPACITY ASSESSMENT OF FRAMED STRUCTURES DAMAGED BY EXCEPTIONAL ACTIONS

A. Formisano[1], G. Iazzetta[2], G. Marino[3], F. Fabbrocino[4] and R. Landolfo[5]

[1,2,3,5]Department of Structures for Engineering and Architecture
Piazzale Tecchio 80, 80125 Naples
e-mail: [1]antoform@unina.it, [2]peppe.iazzetta@libero.it, [3]gmarino1986@libero.it, [5]landolfo@unina.it,

[4]Department of Engineering, Pegaso Telematic University
Centro Direzionale, Isola A3, 80143 Naples
e-mail: [4]francesco.fabbrocino@unipegaso.it

Keywords: Framed structures, Exceptional actions, Fire damage, Seismic response, Residual capacity, Theoretical model.

Abstract. *The effect of natural or man-made disasters, especially when they assume exceptional character, on the urban habitat (buildings, infrastructures, etc.) can result in damages and losses for billions of dollars. In case of cascading events, the residual capacity of a construction damaged from a first threat is not evaluated through suitable calculation procedures neither well codified in actual standards.*

In this framework and with reference to framed structure buildings, the current research activity has the task to provide a tool which helps structural engineers to make a fast evaluation of the buildings performance after exceptional loading actions. Specifically, a theoretical formulation based on the results provided by pushover analyses for the assessment of the residual seismic capacity of buildings after damage produced by exceptional actions is herein presented. The theoretical method presented is basically applied to some case studies of steel framed buildings aiming at showing its effectiveness. To this purpose, a general analysis methodology, with the aim to show the procedure for the practical application of the theoretical formulation, is shown. Such a methodology has been applied to two steel framed buildings designed according to both the old and the new seismic Italian codes. After these frames have been subjected to a fire analysis at different temperatures, non-liner static analyses including P-Δ effects have been carried out with the aim to estimating both the force-displacement curves and the plasticity distribution in the structures. The analyses have provided the tangible application of the procedure, giving the structural parameters accounting for the structure damage status at the end of the exceptional loading action.

.

1   INTRODUCTION

Disasters occur under many different forms and have duration ranging from a hourly disruption to days or weeks of ongoing destruction. They can be either natural [1] or produced by people, both of them having a great impact on the community.

Hurricanes [2, 3] and tropical storms are among the most powerful natural disasters because of their size and destructive potential. Tornadoes are relatively brief but violent and, together with earthquakes, strike suddenly without warning. Flooding is the most common of natural hazards and requires an understanding of the environment natural systems.

Disasters can also be caused by humans. Hazardous materials emergencies include chemical spills and groundwater contamination. Workplace fires are more common and can cause significant property damage and loss of life. Communities are also vulnerable to threats posed by extremist groups, who use violence against both people and property. High-risk targets include military and civilian government facilities, international airports, large cities and high-profile landmarks. Cyber-terrorism involves attacks against computers and networks done to intimidate or coerce a government or its people for political or social objectives.

After constructions are subjected to a first extreme event, the structural performance evaluation should be related to the building response under gravity loads. After this step, the structure should be checked with reference to the seismic actions used in the design phase.

For example, considering fire exposure as a damage event, few studies have been developed and implemented to assess the residual seismic capacity of framed structures after the above exceptional action.

Among the limited researches available in literature, it was found that Mostafei et al. provided a study on the seismic resistance of fire-damaged reinforced concrete columns [4]. Analytical results show that the main seismic resistance properties of two reinforced concrete columns, namely the lateral load capacity and ductility, decreased substantially due to fire exposure. Mostafei also performed a structural test for evaluating the residual lateral load resistance of a reinforced concrete structure after fire damage [5]. Results of this test showed a reduction of both residual lateral stiffness and lateral load capacity of the structure after fire damage.

In the framework of this research activity, in the first part of this study, a theoretical formulation (based on pushover curves) for the assessment of seismic residual capacity of framed structure after extreme load action has been proposed. Instead, in the second part, related to the numerical investigation on moment resisting steel frames after fire damage, an analysis methodology able to validate the equations given in the first part has been proposed.

More in detail, based on the results provided in first part of this paper, with the aim to show a numerical procedure able to evaluate the functions $k_\delta (\phi)$, $k_F (\phi)$ used to measure the reduction of structural performance after an exceptional action, numerical non-linear seismic analyses on two steel structures, before subjected to fire and designed according to both the old [6] and the new [7] seismic Italian codes, have been performed.

2   THEORETICAL PREDICTION OF THE SEISMIC RESPONSE OF DAMAGED FRAMED STRUCTURES

In the last few decades, with the development of Performance-Based Design procedures, the need of simplified methods to estimate with an adequate confidence level the seismic demand for structures is increased. Non-linear static procedures appear as one of the most attractive analysis tool due to both their ease of use and also for the simple and effective graphical representation of the structural response by means of the so-called pushover curve.

The procedure of a conventional pushover analysis [8] is an incremental-iterative solution of the static equilibrium equations. The forcing function is a set of displacements or forces that are necessarily kept constant during the analysis. During an increment of displacement or force, the resistance of the structure is evaluated from the internal equilibrium conditions and the stiffness matrix is updated under certain conditions dependent on the iterative scheme adopted. The unbalanced forces are re-applied if they are deemed large until a convergence criterion is satisfied. At convergence, the stiffness matrix is reorganised and another increment of displacements or forces is applied.

In order to evaluate the seismic capacity of a framed structure before damaged by extreme actions, a theoretical formulation based on the F-δ pushover curve is herein proposed. The proposed formulation allows to evaluate the seismic response by determining three significant points of the cited response curve.

With reference to the Figure 1, which schematically illustrates the results provided by a push-over analysis carried out on a generic undamaged framed structure, it is possible to identify the following points:
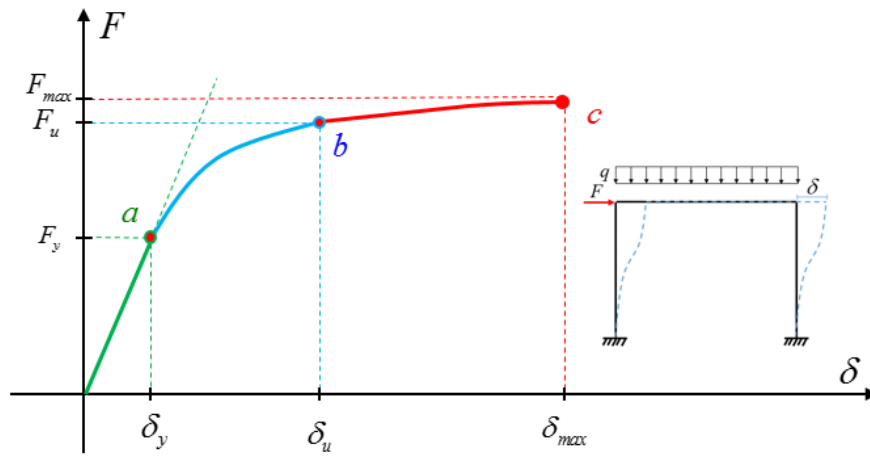

Figure 1: General force-displacement curve.

- Point a (F_y; δ_y) = seismic base shear and top horizontal displacement values corresponding to the first yielding;

- Point b (F_u; δ_u) = seismic base shear and top horizontal displacement values corresponding to the structure excursion in the elasto-plastic field;

- Point c (F_{max}; δ_{max}) = seismic base shear and top horizontal displacement values corresponding to the collapse.

So, when the following conditions are met:

$$F \in \left[0; F_y \right]$$
$$\delta \in \left[0; \delta_y \right]$$

(1)

the structure is in the elastic range.

Instead, when:

$$F \in \left[F_y ; F_u \right]$$
$$\delta \in \left[\delta_y ; \delta_u \right]$$

(2)

the structure is in the elastic-plastic range and, finally, when:

$$F \in \left[F_u; F_{max} \right]$$
$$\delta \in \left[\delta_u; \delta_{max} \right]$$

(3)

the structure is in the plastic range up to the collapse condition (robustness field).

The quantities shown in Figure 1, useful for the assessment of seismic capacity of undamaged framed structure, can also be used to determine the residual capacity of buildings damaged by exceptional loading actions.

To this purpose, the mentioned quantities must be corrected to take into account the damage produced by an extreme load acting before the earthquake. In particular, in order to determine the seismic capacity of a framed structure damaged by an exceptional action, it is necessary to calculate the points a, b and c of the F-δ curve corresponding to each damage level induced by external (natural or man-made) actions. Consequently, the following relationships have to be considered:

$$\begin{cases} F_y \rightarrow F_y(\phi) \\ F_u \rightarrow F_u(\phi) \\ F_{max} \rightarrow F_{max}(\phi) \end{cases}$$

(4)

$$\begin{cases} \delta_y \rightarrow \delta_y(\phi) \\ \delta_u \rightarrow \delta_u(\phi) \\ \delta_{max} \rightarrow \delta_{max}(\phi) \end{cases}$$

(5)

where (F_y, F_u, F_{max}) and (δ_y, δ_u, δ_{max}) are parameters representative of the seismic behaviour of the original structure (without damage), while the corresponding ($F_y(\phi)$, $F_u(\phi)$, $F_{max}(\phi)$) and ($\delta_y(\phi)$, $\delta_u(\phi)$, $\delta_{max}(\phi)$) are indicative of the structural seismic behaviour after induced damage. The parameter ϕ has to be seen as "the value of a generic parameter correlated to a specific damage state produced by an assigned external action acting before the seismic event". Table 1 shows some meanings assumed by the damage parameter ϕ corresponding to different types of exceptional actions considered.

Exceptional Load	Φ
Fire	Temperature, Exposure time [4], [5], [9]
Hurricane, Tornado	Wind speed [2]
Blast load, Explosion	Wave front speed; Peck static overpressure; Maximum dynamic pressure [10], [11], [12]
Volcanic Ash Fall	Ash thickness; Ash density; Ash temperature [13]
Volcanic Pyroclastic Flow	Flow temperature; Flow dynamic pressure; Flow speed [13]
Volcanic Lahar	Lahar speed; Lahar hydrodynamic pressure [13]
Volcanic Earthquake	Earthquake Peak Ground Acceleration (PGA) [13]

Table 1: Examples of damage parameters corresponding to various types of exceptional actions.

Once ϕ is defined and assuming known the values of the following functions:

$$\alpha_y(\phi) = \left[F_y(\phi)/F_y \right]$$
$$\alpha_u(\phi) = \left[F_u(\phi)/F_u \right] \tag{6}$$
$$\alpha_{max}(\phi) = \left[F_{max}(\phi)/F_{max} \right]$$

$$\xi_y(\phi) = \left[\delta_y(\phi)/\delta_y \right]$$
$$\xi_u(\phi) = \left[\delta_u(\phi)/\delta_u \right] \tag{7}$$
$$\xi_{max}(\phi) = \left[\delta_{max}(\phi)/\delta_{max} \right]$$

the values of displacements and forces after damage can be expressed in the following way:

$$\delta_y(\phi) = \delta_y \cdot \xi_y(\phi)$$
$$\delta_u(\phi) = \delta_u \cdot \xi_u(\phi) \tag{8}$$
$$\delta_{max}(\phi) = \delta_{max} \cdot \xi_{max}(\phi)$$

$$F_y(\phi) = F_y \cdot \alpha_y(\phi)$$
$$F_u(\phi) = F_u \cdot \alpha_u(\phi) \tag{9}$$
$$F_{max}(\phi) = F_{max} \cdot \alpha_{max}(\phi)$$

From these general relationships it is possible to extrapolate a more compact formulation, thereby expressing the six constants (F_y, F_u, F_{max}, δ_y, δ_u, δ_{max}) as a function of only two maximum parameters (F_{max}, δ_{max}) of the curve. This is shown in Figure 2, where the dimensionless pushover curve obtained for a generic ϕ parameter is plotted.
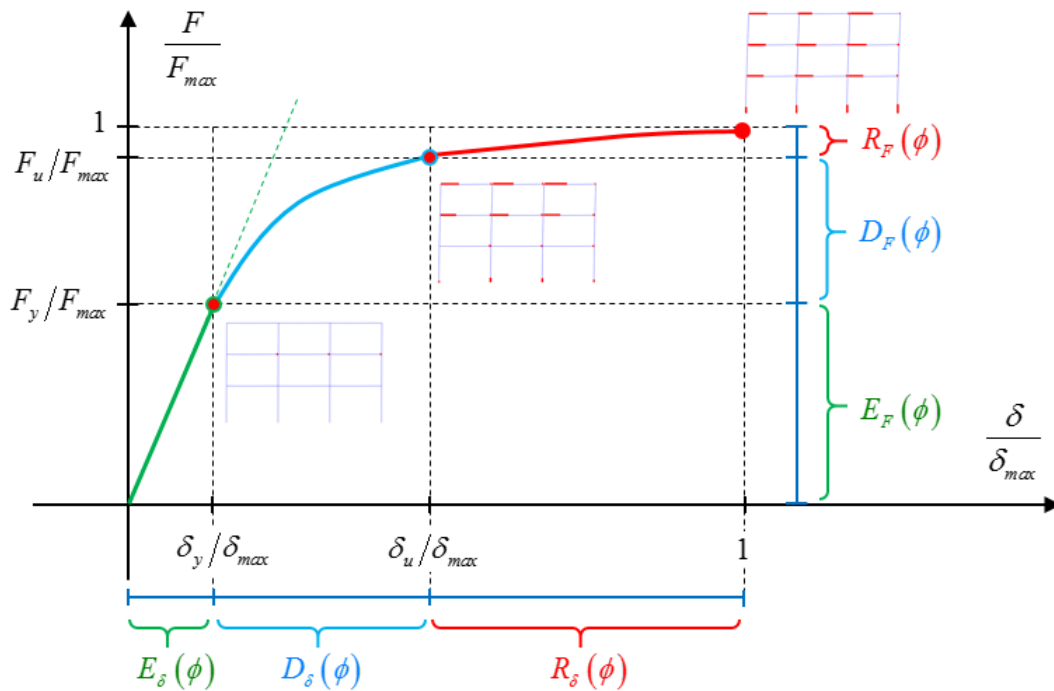

Figure 2: Dimensionless pushover curve.

Assuming once again known the functions described in equations (6) and (7), it is possible to write:

$$E_\delta\left(\phi\right)=\left[\frac{\delta_y}{\delta_{max}}\cdot\frac{\xi_y\left(\phi\right)}{\xi_{max}\left(\phi\right)}\right] \tag{10}$$

$$D_\delta\left(\phi\right)=\left\{\left[\frac{\delta_u}{\delta_{max}}\cdot\frac{\xi_u\left(\phi\right)}{\xi_{max}\left(\phi\right)}\right]-\left[\frac{\delta_y}{\delta_{max}}\cdot\frac{\xi_y\left(\phi\right)}{\xi_{max}\left(\phi\right)}\right]\right\} \tag{11}$$

$$R_\delta\left(\phi\right)=\left\{1-\left[\frac{\delta_u}{\delta_{max}}\cdot\frac{\xi_u\left(\phi\right)}{\xi_{max}\left(\phi\right)}\right]\right\} \tag{12}$$

These functions must satisfy the following conditions:

$$\begin{cases}E_\delta\left(\phi\right)\\ D_\delta\left(\phi\right)\in\left[0;1\right]:\to E_\delta\left(\phi\right)+D_\delta\left(\phi\right)+R_\delta\left(\phi\right)=1\\ R_\delta\left(\phi\right)\end{cases} \tag{13}$$

$E_\delta\left(\phi\right)$, $D_\delta\left(\phi\right)$ and $R_\delta\left(\phi\right)$ are parameters that can be seen as distribution coefficients of the seismic capacity of structures in terms of horizontal displacement. In particular, $E_\delta\left(\phi\right)$ refers to the elastic field, $D_\delta\left(\phi\right)$ to the ductile field and $R_\delta\left(\phi\right)$ to the robustness field.

Multiplying the expressions (10), (11) and (12) for the quantity ($\delta_{max}\cdot\xi_{max,}$), the following equations can be derived:

$$\delta_{max}\cdot\xi_{max}\left(\phi\right)\cdot E_\delta\left(\phi\right)=\Delta\delta_y\left(\phi\right) \tag{14}$$

$$\delta_{max}\cdot\xi_{max}\left(\phi\right)\cdot D_\delta\left(\phi\right)=\Delta\delta_u\left(\phi\right) \tag{15}$$

$$\delta_{max}\cdot\xi_{max}\left(\phi\right)\cdot R_\delta\left(\phi\right)=\Delta\delta_{max}\left(\phi\right) \tag{16}$$

where $\Delta\delta_i(\phi)$ (i=y, u, max) are the displacement increment necessary for the transition from a behavioural phase to the following one.

Through the equations (14), (15) and (16), it is possible to write:

$$\delta_y\left(\phi\right)=0+\Delta\delta_y\left(\phi\right) \tag{17}$$

$$\delta_u\left(\phi\right)=\delta_y\left(\phi\right)+\Delta\delta_u\left(\phi\right) \tag{18}$$

$$\delta_{max}\left(\phi\right)=\delta_u\left(\phi\right)+\Delta\delta_{max}\left(\phi\right) \tag{19}$$

where $\delta_i(\phi)$ (i=y,u,max) are the basic displacements required to determine the seismic response in the displacement field.

Placing the equations (14), (15), (16) in the equations (17), (18), (19), it is possible to write:

$$\delta_y\left(\phi\right)=0+\delta_{max}\cdot\xi_{max}\left(\phi\right)\cdot E_\delta\left(\phi\right) \tag{20}$$

$$\delta_u\left(\phi\right)=\left[\delta_{max}\cdot\xi_{max}\left(\phi\right)\cdot E_\delta\left(\phi\right)\right]+\left[\delta_{max}\cdot\xi_{max}\left(\phi\right)\cdot D_\delta\left(\phi\right)\right] \tag{21}$$

$$\delta_{max}\left(\phi\right)=\left[\delta_{max}\cdot\xi_{max}\left(\phi\right)\cdot E_\delta\left(\phi\right)\right]+\left[\delta_{max}\cdot\xi_{max}\left(\phi\right)\cdot D_\delta\left(\phi\right)\right]+\left[\delta_{max}\cdot\xi_{max}\left(\phi\right)\cdot R_\delta\left(\phi\right)\right] \tag{22}$$

Grouping the equations (20), (21) and (22) with respect to ($\delta_{max} \cdot \xi_{max}(\phi)$), the following relationships are achieved:

$$k_{y,\delta}(\phi) = \xi_{max}(\phi) \cdot E_\delta(\phi) \tag{23}$$

$$k_{u,\delta}(\phi) = \xi_{max}(\phi) \cdot \left[E_\delta(\phi) + D_\delta(\phi) \right] \tag{24}$$

$$k_{max,\delta}(\phi) = \xi_{max}(\phi) \cdot \left[E_\delta(\phi) + D_\delta(\phi) + R_\delta(\phi) \right] = \xi_{max}(\phi) \tag{25}$$

where $k_{i,\delta}(\phi)$ (i= y, u, max) are the reduction factors of seismic performance of the structure in the displacement field, which take implicitly into account the repartition of the capacity itself.

Definetively, it is possible to write:

$$\delta_y(\phi) = \left[\delta_{max} \cdot k_{y,\delta}(\phi) \right] \tag{26}$$

$$\delta_u(\phi) = \left[\delta_{max} \cdot k_{u,\delta}(\phi) \right] \tag{27}$$

$$\delta_{max}(\phi) = \left[\delta_{max} \cdot k_{max,\delta}(\phi) \right] \tag{28}$$

Instead the equations (26), (27) and (28) show that the basic displacements $\delta_y(\phi)$, $\delta_u(\phi)$ and $\delta_{max}(\phi)$ belonging to the $F(\phi)$–$\delta(\phi)$ curve can be calculated starting from the displacement value δ_{max} only, therefore neglecting the δ_u and δ_y values.

Equivalently, the trends of $F_y(\phi)$, $F_u(\phi)$ and $F_{max}(\phi)$ can be expressed as a function of the F_{max} value only by considering the $k_{F,y}(\phi)$, $k_{F,u}(\phi)$ and $k_{F,max}(\phi)$ parameters as follows:

$$F_y(\phi) = \left[F_{max} \cdot k_{y,F}(\phi) \right] \tag{29}$$

$$F_u(\phi) = \left[F_{max} \cdot k_{u,F}(\phi) \right] \tag{30}$$

$$F_{max}(\phi) = \left[F_{max} \cdot k_{max,F}(\phi) \right] \tag{31}$$

where:

$$k_{y,F}(\phi) = \alpha_{max}(\phi) \cdot E_F(\phi) \tag{32}$$

$$k_{u,F}(\phi) = \alpha_{max}(\phi) \cdot \left[E_F(\phi) + D_F(\phi) \right] \tag{33}$$

$$k_{max,F}(\phi) = \alpha_{max}(\phi) \cdot \left[E_F(\phi) + D_F(\phi) + R_F(\phi) \right] = \alpha_{max}(\phi) \tag{34}$$

Definitively, all the previous relationships provide a theoretical formulation for the calculation of the seismic response of a framed structure previously damaged by an extreme event.

Unfortunately, into equations (8), (9), (26), (27), (28), (29), (30) and (31), the values of the functions $\alpha(\phi)$, $\xi(\phi)$, $k_\delta(\phi)$ and $k_F(\phi)$ are not known a priori (see respectively equations (6), (7), (23), (24), (25), (32), (33), (34)) .

Basically, the main issue consists on the determination of the structure damage status at the end of the exceptional loading action. In this framework, Table 2 shows some of the variables, other than the building properties, which influence the structural response.

Exceptional Load	Influential variables
Fire	Fire scenario, Fire model, Fire Proofing
Hurricane, Tornado	Wind speed
Blast load, Explosion	Explosive characteristic, Detonation scenario, Blast Proofing
Volcanic Ash Fall	Ash thickness, Ash density, Ash temperature , Roof configuration
Volcanic Pyroclastic Flow	Flow dynamic pressure, Building shape, Topographical configuration of the site
Volcanic Lahar	Structural typology, Impact Angle with structure, Lahar temperature, Impact surface, Flow density
Volcanic Earthquake	Earthquake Response Spectrum, Soil-Structure Interaction.

Table 2: List of various variables influencing different types of exceptional actions.

The variables listed into the above table must be considered in order to provide useful values of the functions $\alpha\,(\phi)$ and $\xi\,(\phi)$ and, consequently, of the functions $k_\delta\,(\phi)$ and $k_F\,(\phi)$ for design purposes. This aim can be accomplished through a comprehensive numerical and experimental investigation campaign by taking into account at least the variability of the above mentioned influential variables.

Once known these functions and the undamaged structure capacity (F_{max}; δ_{max}), a simplified check of the seismic capacity of a given framed structure after an exceptional loading action can be executed without performing sequential non-linear analyses.

3 THE CASE STUDIES

In order to show the effectiveness of the theoretical method presented above, starting from the general equations described in Section 2, it can be possible to replace the dependence of the functions from "ϕ" with the specified damage parameter that, in the specific case, consists on the temperature value "θ" inside the structural members.

Practically, starting from the following general equations:

$$F\left(\phi\right) = F_{max} \cdot k_F\left(\phi\right)$$
$$\delta\left(\phi\right) = \delta_{max} \cdot k_\delta\left(\phi\right)$$

(35)

it is possible to express the study significant parameters as a function of the parameter θ as follows:

$$\alpha\left(\phi\right) \to \alpha\left(\theta\right)$$
$$\xi\left(\phi\right) \to \xi\left(\theta\right)$$

(36)

$$k_F\left(\phi\right) \to k_F\left(\theta\right)$$
$$k_\delta\left(\phi\right) \to k_\delta\left(\theta\right)$$

(37)

which give rise to the following relationships:

$$F(\phi) = F_{max} \cdot k_F(\theta)$$
$$\delta(\phi) = \delta_{max} \cdot k_\delta(\theta)$$

(38)

that are used to examine the structural seismic behaviour of steel MRF after fire.

3.1 Geometrical and mechanical features

In this study, two different types of steel framed structures have been analysed aiming at evaluating their seismic capacity after fire actions. The choice of the frame types has been done according to a previous study performed by the first Author [14, 15, 16].

The first framed structure has been designed according to the old Seismic Italian Code (M.D., 1996), while the second one has been designed according to the new Seismic Italian Code (M.D., 2008). Both structures are subjected to permanent and variable loads of 5.15 kNm^{-2} and 2 kNm^{-2}, respectively.

Both framed structures have the same geometric configuration with three 5m bays and three levels (H=3.50 m at 1st floor; H=3.00 m at 2nd and 3rd floor).

Figure 3 shows the geometrical properties of the steel framed structures inspected.
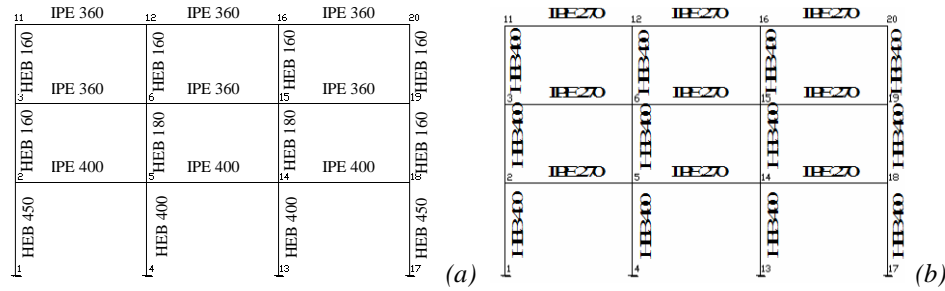
Figure 3: The examined steel framed structures designed according to M.D. 1996 (a) and M.D. 2008 (b).

The selected framed buildings are made of S275JR steel profiles.

Figure 4a shows the stress-strain relationships of the steel material used in this study, while figure 4b shows the reduction factors of the material mechanical properties at elevated temperatures [17].

In particular, six uniform temperature fields (θ= 20°C, 100°C, 200°C, 300°C, 400°C, 500°C) have been applied to the structures before seismic loads have been considered.
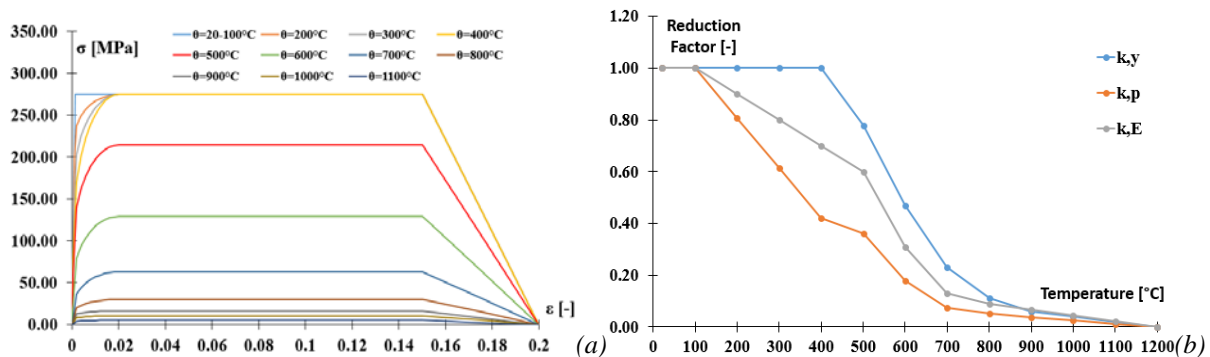

Figure 4: Mechanical properties of S275JR steel: constitutive laws (a) and reduction factors (b) at different temperatures.

3.2 The FEM models

Non-linear static analyses including *P-Δ* effects have been performed by means of the FE software "ABAQUS v.6.10-1" [18] in order to estimate both the force-displacements pushover curves and the plasticity distribution in the inspected structures.

Figure 5a and b show the details of the typical finite element model based on beam elements used for modelling the generic frame. In particular, columns and beams have been modelled by using into a 2D model the beam elements type B21. Second-order elements, like B22 ones, have been avoided owing to the so-called 'volumetric locking' problem, which is induced by the large strains in the frame deformed configuration. Firstly, the effect of different number of constitutive elements for columns and beams has been investigated in order to provide accurate results with a reduced computational time. It was found that 80 elements are sufficient for a reliable analysis of the 2D plane frame model.
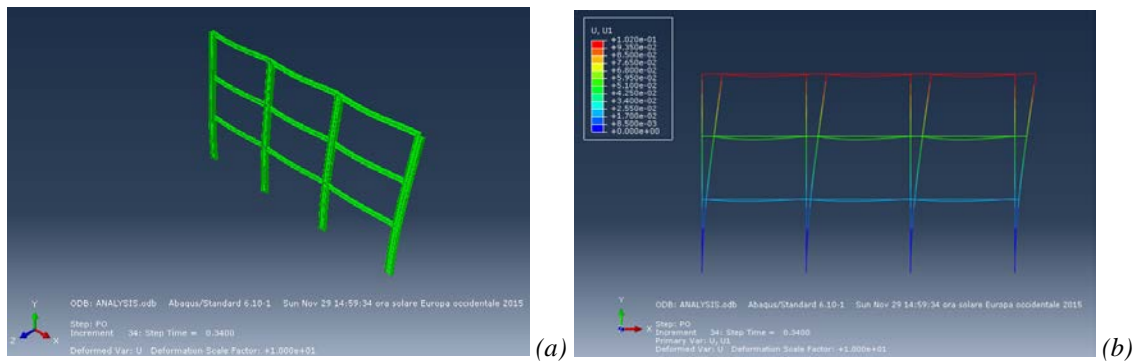

Figure 5: Deformed FEM model under gravity loads of one of the tested frames (a) and horizontal displacements under seismic actions (b).

The column bases of the steel framed structures are fixed (fully rigid column bases). For the sake of simplicity, rotational stiffness of beam-column joints have not been modelled, but the full continuity between beams and columns at their intersections has been considered. In the Abaqus numerical models, the non-linear stress-strain material curves have been modelled. Since the analysis involves large inelastic strains, the engineering stress-strain curves have been converted into true stresses vs. logaritmic plastic strains at different temperatures. In fact, in order to simulate the effect of fire, a simplified hypothesis has been done: only the mechanical property variation has been considered, neglecting thermal expansions and the related phenomena. So, mechanical properties change due to temperature has been considered constant through the cross-sections and applied to all structural members.

3.3 Numerical results at θ = 20 - 100°C

The analyses performed with the Abaqus software on the examined structures at the environment condition (θ = 20°C) have shown that their behaviour is analogous to that of the same structures at θ = 100°C. The numerical analysis results in the non-linear field on the case studies in terms of diplacements and force-displacement pushover curves are illustrated in Figures 6a and b, respectively.
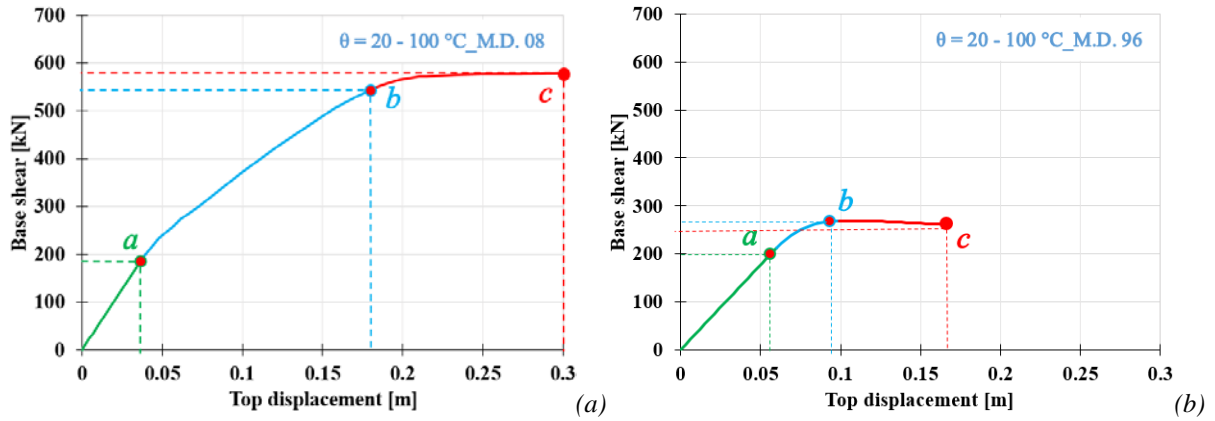
Figure 6: Force-displacement pushover curves at θ = 20 – 100°C for frames designed with M.D. 08 (a) and M.D. 96 (b) codes.

The points highlighted in Figure 6 have been determined starting from the study of plasticity distribution within the structures subjected to horizontal incremental loads [19, 20]. In order to better understand this aspect, firstly reference is made to the Figures 7a and 8a, where the damage state corresponding to the first yelding phenomena due to horizontal loads in the structures designed according to M.D. 08 and M.D. 96, respectively, is plotted. This plasticity distribution corresponds to the points "a" of the force-displacement curves of Figures 6a and 6b.
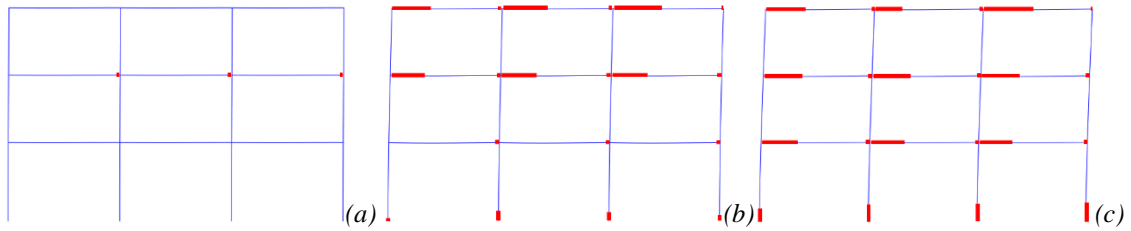

Figure 7: Plasticity distribution at θ = 20 – 100°C for the M.D. 08 frame: (a) first yielding; (b) mechanism activation; (c) collapse.
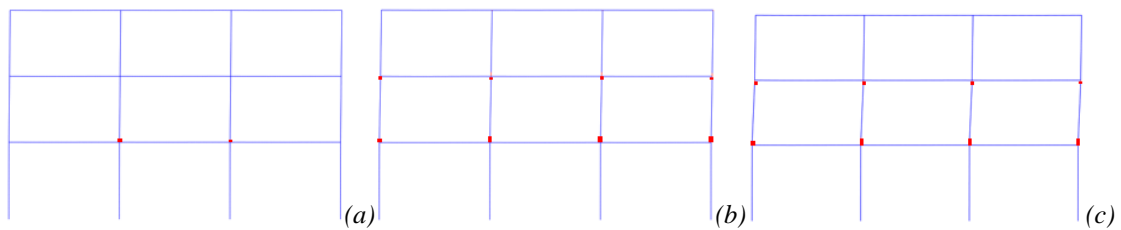

Figure 8: Plasticity distribution at θ = 20 – 100°C for the M.D. 06 frame: (a) first yielding; (b) mechanism activation; (c) collapse.

Figures 7b and 8b provide a snapshot of the plasticity distribution at the time of the mechanism activation for M.D. 08 frame and M.D. 96 one, respectively. This condition is reached when a quasi-global collapse mechanism for M.D. 08 frame and a soft-storey mechanism for M.D. 96 frame are attained. In this condition, the points "b" of the curves in Figures 6a and 6b are reached.

Finally, Figures 7c and 8c show the distribution and the extension of the yielded zone at collapse for the examined structures. This condition occurs when the extension of the plastic zones in the columns is equal to the cross-section height. Therefore, the parameters F_{max} and δ_{max} are attained, they providing the points "c" of the curves in Figures 6a and 6b.

3.4   Numerical results at high temperatures

Following the procedure described in the previous section and considering different temperature values up to 500°C, the non-linear force-displacement curves of the investigated frames have been obtained. These curves, which are representative of the seismic capacity of the Italian frames under examination, are shown in Figures 9a and 9b.
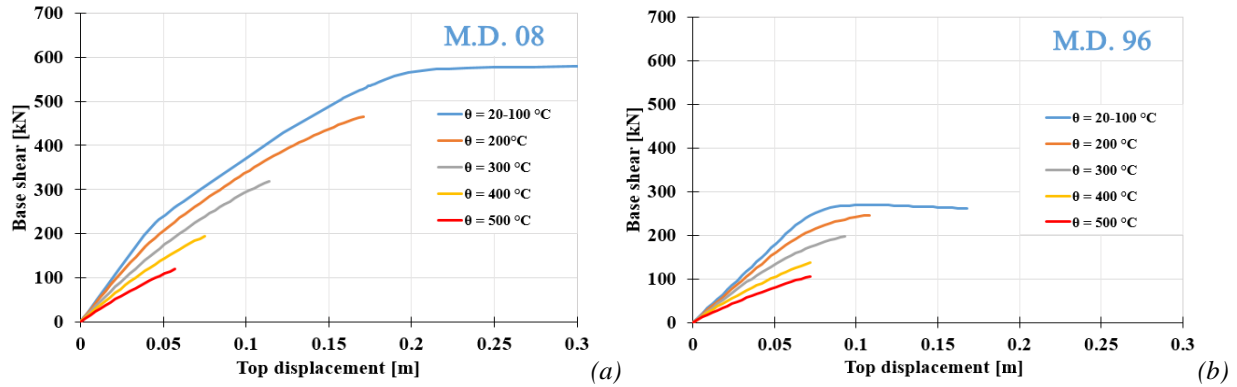

Figure 9: Force-displacement curves obtained from non-linear analyses on M.D. 08 (a) and M.D. 96 (b) frames.

The analysis of results describing the plasticity evolution within the study framed structures has allowed to redact the Tables 3 and 4, where the lists of variables describing the seismic response curves are plotted. In such tables, the zero values are indicative of the incapacity of structures to withstand seismic actions after fire.

From the analysis of results, it is highlighted that, at the same value of temperature, a substantial behavioural difference between the framed structure designed according to the new Seismic Italian Code (M.D., 2008) and the one designed according to the old Seismic Italian Code (M.D., 1996) exists.

M.D. 08						
θ [°C]	F_y [kN]	F_u [kN]	F_{max} [kN]	δ_y [m]	δ_u [m]	δ_{max} [m]
20	196.12	543.75	579.00	0.0386	0.180	0.300
100	196.12	543.75	579.00	0.0386	0.180	0.300
200	83.40	422.47	466.10	0.0180	0.141	0.170
300	0	297.10	319.50	0	0.104	0.114
400	0	177.70	192.20	0	0.066	0.075
500	0	120.00	120.00	0	0.060	0.060

Table 3: Numerical results obtained from analyses on the structure designed according to the M.D. 08 code.

M.D. 96						
θ [°C]	F_y [kN]	F_u [kN]	F_{max} [kN]	δ_y [m]	δ_u [m]	δ_{max} [m]
20	212.99	269.12	261.10	0.060	0.099	0.168
100	212.99	269.12	261.10	0.060	0.099	0.168
200	143.43	230.58	246.00	0.045	0.087	0.108
300	76.34	177.57	198.33	0.027	0.075	0.093
400	22.25	129.13	137.14	0.009	0.066	0.072
500	0	103.13	108.80	0	0.066	0.072

Table 4: Numerical results obtained from analyses on the structure designed according to the M.D. 96 code.

In order to quantify the above detected differences, the pictures reported in Figures 10a and 10b need to be considered.
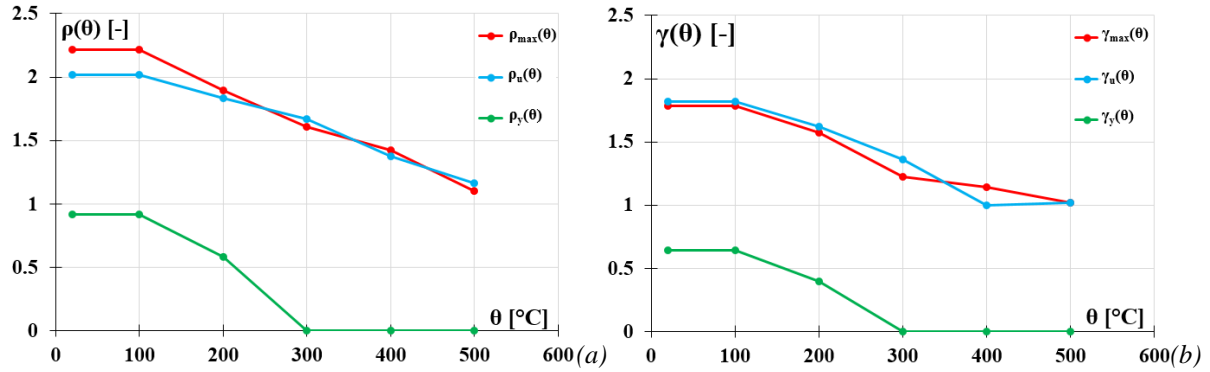

Figure 10: Behavioural trends of the $\rho - \theta$ (a) and $\gamma - \theta$ (b) curves.

The above graphs are representative of the following functions:

$$\rho_y(\theta) = \left[F_y(\theta)_{M.D.08} \Big/ F_y(\theta)_{M.D.96} \right]$$

$$\rho_u(\theta) = \left[F_u(\theta)_{M.D.08} \Big/ F_u(\theta)_{M.D.96} \right] \tag{39}$$

$$\rho_{max}(\theta) = \left[F_{max}(\theta)_{M.D.08} \Big/ F_{max}(\theta)_{M.D.96} \right]$$

$$\gamma_y(\theta) = \left[\delta_y(\theta)_{M.D.08} \Big/ \delta_y(\theta)_{M.D.96} \right]$$

$$\gamma_u(\theta) = \left[\delta_u(\theta)_{M.D.08} \Big/ \delta_u(\theta)_{M.D.96} \right] \tag{40}$$

$$\gamma_{max}(\theta) = \left[\delta_{max}(\theta)_{M.D.08} \Big/ \delta_{max}(\theta)_{M.D.96} \right]$$

From the reported trends it can be observed that, at the same temperature, structure designed according to the M.D. 08 code always shows a seismic performance in the elastic-plastic and plastic ranges greater than that of the frame designed according to the M.D. 96 code. This occurs in terms of both forces and displacements up to 400 °C.

Analogously to the design philosophy at basis of the two codes, the detected situation changes in the elastic range. In fact, it can be noted that the M.D. 96 frame, being designed to remain mainly in the elastic range under applied loads, has shown an elastic performance better than that of the M.D. 08 frame, which is designed particularly to dissipate the amount of the seismic energy input in the elastic-plastic range, showing greater excursions in the plastic field. To confirm this, it can be observed that, starting from a temperature of 300 °C, the formation of plastic zones in the M.D. 08 structure occurs already for vertical loads, while this condition for the other structure happens at a temperature of 500 °C.

Regarding the degradation of forces and displacements with the temperature, reference is made to the trends shown in Figures 11a and 11b, which represent the functions described in the equation (6), for M.D.08 frame and M.D. 96 one, respectively. On the other hand, the variation of the parameter ξ with temperature θ is shown in Figures 12a and 12b.

As it can be observed, at the same temperature, force and displacement parameters undergo significant reductions, particularly in the elastic field, for the structure designed according to the M.D. 08 code.

This condition can be explained considering the reduced seismic capacity of the old structure compared to the new one, as well as the different collapse mechanisms attributable to the two structures analysed (floor mechanism for the M.D. 96 frame and column

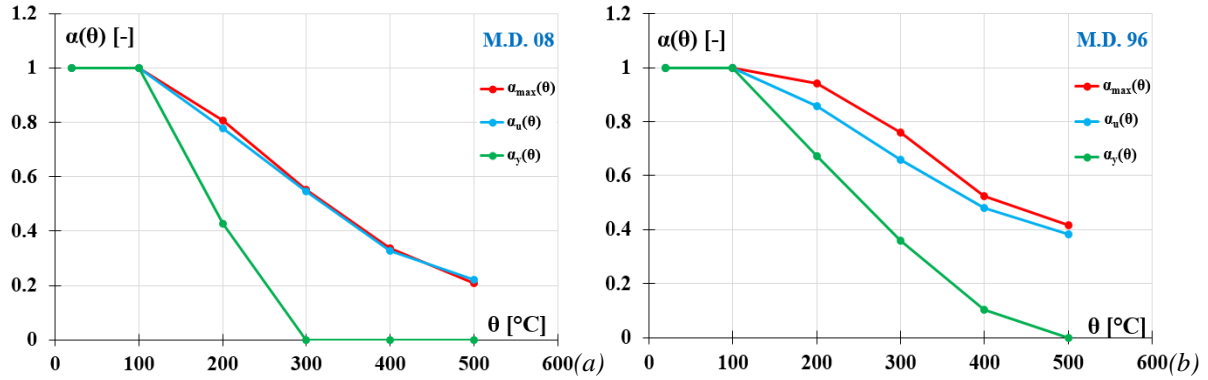mechanism at their base for the M.D. 08 frame, neglecting in both cases the beam mechanisms).

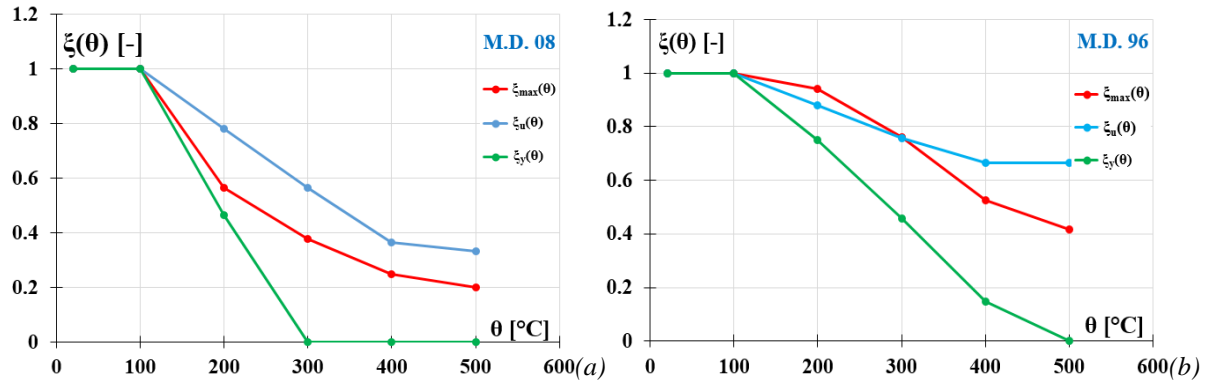Figure 11: $\alpha - \theta$ curves for M.D. 08 (a) and M.D. 96 (b) frames.

Figure 12: $\xi - \theta$ curves for M.D. 08 (a) and M.D. 96 (b) frames.

3.5 Calculation of $k_F(\theta)$ and $k_\delta(\theta)$ functions

Starting from the results provided by the numerical analyses performed on the two steel frames, the functions described by equations (6) and (7) in Section 2 have been calculated.

Once evaluated the pushover response parameters at θ=20°C, combining them with the functions cited above, the $k_F(\theta)$ and $k_\delta(\theta)$ functions are achieved.

Figures 13, 14 and 15 show the trends of the functions described above for the two frames designed with different seismic design codes.
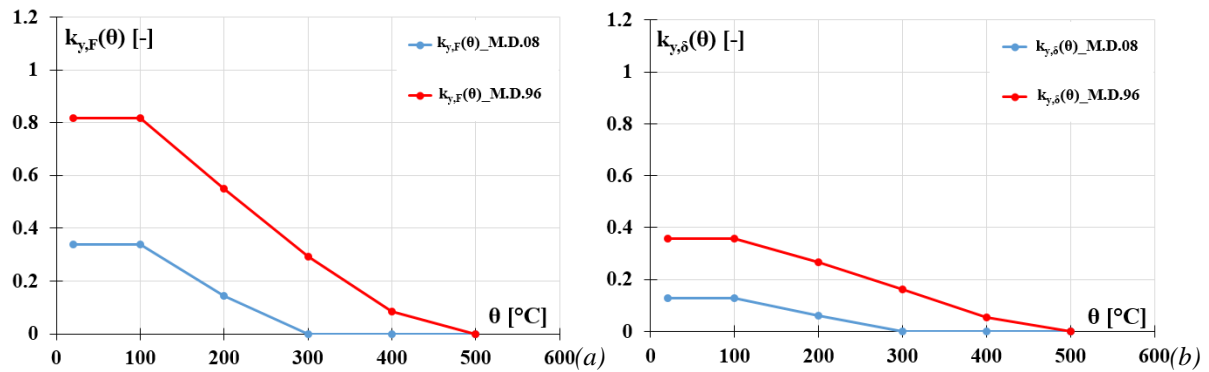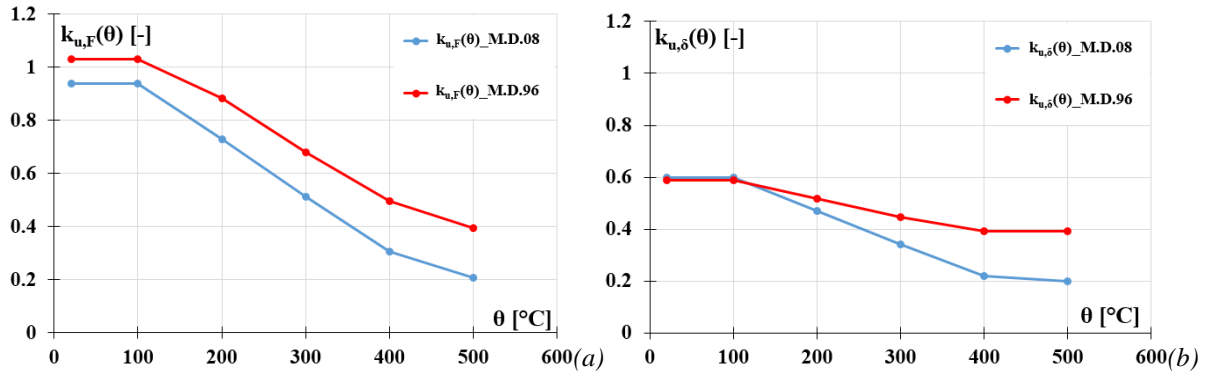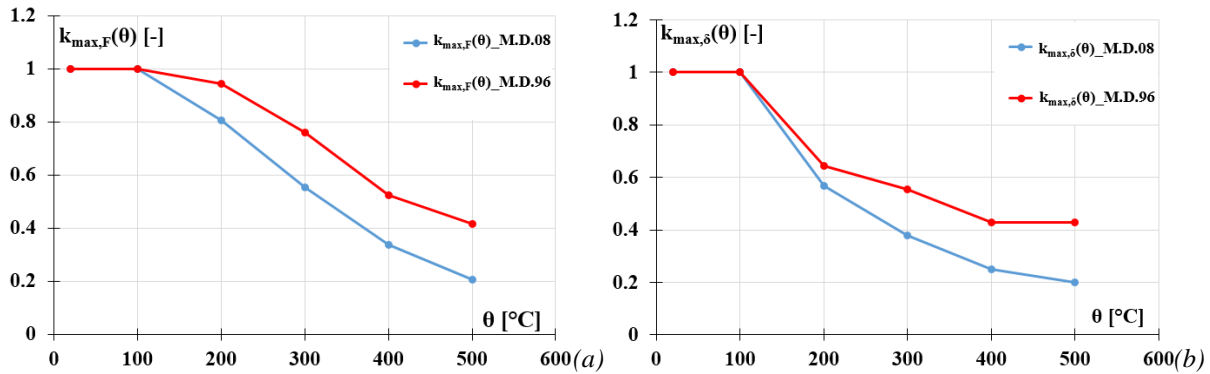

Figure 13: $k_{y,F} - \theta$ (a) and $k_{y,\delta} - \theta$ (b) curves of the inspected framed structures.

Figure 14: $k_{u,F} - \theta$ (a) and $k_{u,\delta} - \theta$ (b) curves of the inspected framed structures.

Figure 15: $k_{max,F} - \theta$ (a) and $k_{max,\delta} - \theta$ (b) curves of the inspected framed structures.

As already detected in the previous section for the functions $\xi(\theta)$ and $\alpha(\theta)$, at the same temperature, the most significant reduction of the functions k_δ and k_F with the temperature θ, especially in the elastic field, is detected for the M.D. 08 frame.

Finally, it should be noted that, by multiplying the values of F_{max} and δ_{max} at 20°C for the appropriate values of the above functions, it is possible to fully reconstruct the values of Tables 3 and 4.

4 CONCLUSIVE REMARKS AND FURTHER DEVELOPMENTS

In this study, a research activity concerning the seismic behaviour of framed structures after damages deriving from application of an exceptional load has been carried out.

Based on the results of a pushover analysis, a theoretical formulation to evaluate a simplified force-displacement curve for seismic appraisement of a structure damaged from an extreme event is reported.

However, after the basic non-linear behaviour of the undamaged structure is estimated, the concrete application of the method requires the *a priori* knowledge of some functions depending on the structure damage status at the end of the exceptional loading action. This can be attained by means of a widespread experimental-numerical examination campaign for evaluating the damages deriving from some variables influencing the effects of a given exceptional action.

An effective and practical way to apply the proposed method is provided in the Section 3 of the paper, where the residual seismic capacity of steel Moment Resisting Frames (designed according to both the new and the old seismic Italian codes) subjected to a preliminary fire action is estimated.

Numerical analysis results have shown that the reduction of mechanical properties of steel material due to fire can drastically affect the seismic response of investigated structures.

Results of this numerical investigation have shown that the structure designed according to the M.D. 08 code shows a seismic capacity in the post-elastic range greater than that designed according to the M.D. 96 code. Contrary, in the elastic field, the old frame behaves better than the new one. This is mainly due to the different design approaches used for the inspected frames. In fact the M.D. 96 structure is mainly designed to withstand applied loads without energy dissipation in the post-elastic range (no "capacity design" approach). This means that the first yielding in the old structure develops for base shear values greater than the new frame ones.

Finally, it is perceived that at the room temperature, the base shear capacity of the M.D. 08 frame is at least two times greater than the M.D. 96 structure one. Starting from this condition, the difference between the base shears drastically decreases after fire action. However, it can be noted that the force reduction trend shows a linear gradient with temperature, reaching its lower value at the temperature of 500 °C. The same behaviour is also observed for displacements. These trends are mainly due to the different distribution of damage under seismic loads, which appears to be more distribuited for the M.D. 08 frame, while it is localised at a certain storey for the M.D. 96 structure.

As a further development of the research activity, in order to both better understand the seismic behaviour of steel MRF before and after fire and validate the theoretical formulations given, an exhaustive campaign of numerical and experimental investigations is strongly needed. Some of the aspects that need to be more investigated are:

- The influence of the structure seismic response before fire damage, taking into account different geometrical configurations and any structural irregularities.
- The influence of the fire model and location.
- The influence of structural response at high temperatures, i.e. thermal expansions and related phenomena, as well as the actual temperature distribution in the cross-sections and along the structural elements.

REFERENCES

[1] Raizer V., Natural disasters and structural survivability, *R&RATA #3 (Vol.2)*, San Diego , California. September, 2009.

[2] Yue Li, Ellingwood Bruce R., Hurricane damage to residential construction in the US: Importance of uncertainty modeling in risk assessment, *Engineering Structures 28 pp. 1009-1018, Elsevier.* 2006.

[3] Jordan James W. and Paulius Saul L., Lessons Learned from Hurricane Katrina, *American Society of Civil Engineers (ASCE)*, Proceedings of the Fourth Forensic Engineering Congress, held in Cleveland, Ohio from October 6-9, 2006

[4] Mostafei H., Vecchio F.J., Benichou N., Seismic resistance of fire damaged reinforced concrete columns, Conference on Improving the Seismic Performance of Existing Buildings and other structures, by *the Applied Technology Council and the Structural Engineering Institute of ASCE,* San Francisco, pp 12. December 9-11, 2009.

[5] Mostafei H., A new testing Capability for Seismic Resistance Assessment of Structures Damaged Due to a Fire, *15 WCEE LISBOA*, 2012.

[6] Ministerial Decree of Public Works (M. D.), Technical codes for constructions in seismic zones (in Italian), *Official Gazette of the Italian Republic published on January 16th*, 1996.

[7] Ministerial Decree of Public Works emanated on 2008, January 14th (M.D. 08), New technical codes for constructions (in Italian), *Official Gazette of the Italian Republic n. 29 published on 2008 February 4th*, 2008.

[8] Elnashai Amr S., Advanced inelastic static (pushover analysis for earthquake applications, *Structural Engineering & Mechanics pp. 51-69*, July, 2001

[9] Nigro E., Cefarelli G., Pustorino S., Princi P., Progettazione di strutture in acciaio e composte acciaio-calcestruzzo in caso di incendio secondo gli Eurocodici e le Norme Tecniche per le costruzioni, Hoepli, 2010.

[10] Draganić H., Sigmund V., Blast loading on structures, *Technical Gazette 19,* pp. 643-652. March, 2012.

[11] Luccioni B.M., Ambrosini R.D., Danesi R.F., Analysis of building collapse under blast load, *Engineering Structures 26 pp. 63-71, Elsevier.* 2004.

[12] Ngo T., Mendis P., Gupta A., Ramsay J., Blast loading and blast effect on structures-An overwiew, *EJSE International Special Issue: Loading on structures pp. 76-91*, 2007.

[13] De Gregorio D., Mazzolani F.M., Faggiano B., Vulnerabilità vulcanica dei centri urbani in zone ad elevato rischio: il caso Vesuvio, *Tesi di dottorato in Ingegneria delle Costruzioni XIII ciclo*, 2010.

[14] Formisano A., Mazzolani F.M., On the catenary effect of steel buildings, *Proc. of the COST ACTION C26 Final Conference "Urban Habitat Constructions under Catastrophic Events"*, Naples, Italy, 16-18 September, pp. 619-624, 2010.

[15] Formisano A., Mazzolani F.M., Progressive collapse and robustness of steel framed structures, *Civil-Comp Proceedings*, paper 99, 2012.

[16] Formisano A., Landolfo R., Mazzolani F.M., Robustness assessment approaches for steel framed structures under catastrophic events, *Computers and Structures*, 147, pp. 216-228, 2015.

[17] EN 1993-1-2, *Eurocode 3 – Design of steel structures – Part 1-2: General Rules-Structural Fire Design*, April, 2005.

[18] Simulia, *Abaqus Analysis User's Manual (version 6.10-1)*, Dassault Systemés, Vélizy-Villacoublay, France, 2010.

[19] Formisano A., Faggiano B., Landolfo R., Mazzolani F.M., Ductile behavioural classes of steel members for seismic design, *Proc. of the 5th Int. Conference on Behaviour of Steel Structures in Seismic Areas (Stessa 2006)*, Yokohama, Japan, 14-17 August, pp. 225-232, 2006.

[20] Formisano A., Gamardella F., Mazzolani F.M., Capacity and demand ductility for shear connections in steel MRF structures, *Civil-Comp Proceedings,* paper 102, 2013.